Published in final edited form as:
Brain Res. 2008 September 16; 1230: 273–280. doi:10.1016/j.brainres.2008.06.124.

Hippocampal RAGE Immunoreactivity in Early and Advanced Alzheimer's Disease

Miles C. Miller[1,2], **Rosemarie Tavares**[1], **Conrad E. Johanson**[2], **Virginia Hovanesian**[3], **John E. Donahue**[1], **Liliana Gonzalez**[4], **Gerald D. Silverberg**[2], and **Edward G. Stopa**[1]

1 *Division of Neuropathology, Department of Pathology, Rhode Island Hospital and the Warren Alpert Medical School of Brown University, Providence, RI, USA*

2 *Department of Clinical Neuroscience, Rhode Island Hospital and the Warren Alpert Medical School of Brown University, Providence, RI, USA*

3 *Core Image Analysis Laboratory, Rhode Island Hospital, Providence, RI, USA*

4 *Department of Computer Science and Statistics, University of Rhode Island, Kingston, RI, USA*

Abstract

Microvascular accumulation and neuronal overproduction of amyloid-β peptide (Aβ) are pathologic features of Alzheimer's disease (AD). In this study, we examined the receptor for advanced glycation endproducts (RAGE), a multi-ligand receptor found in both neurons and cerebral microvascular endothelia that binds Aβ. RAGE expression was assessed in aged controls (n=6), patients with early AD-like pathology (n=6), and severe, Braak V-VI AD (n=6). Human hippocampi were stained with a specific polyclonal antibody directed against RAGE (Research Diagnostics, Flanders, NJ). Immunoreactivity was localized in both neurons and cerebral endothelial cells. Quantitative image-analyses were performed on grayscale images to assess the total surface area of endothelial RAGE immunoreaction product in cross sections of cerebral microvessels (5–20 μm). Confocal images were acquired for confirmation of RAGE immunoreactivity in both microvessels and neurons by coupling RAGE with CD-31 and neurofilament, respectively. A significant increase in endothelial RAGE immunoreactivity was found in severe Braak V-VI AD patients when compared to aged controls ($p<0.001$), and when compared to patients with early AD pathology ($p=0.0125$). In addition, a significant increase in endothelial RAGE immunoreactivity was witnessed when comparing aged controls having no reported AD pathology with patients having early AD-like pathology ($p=0.038$). Our data suggest that microvascular RAGE levels increase in conjunction with the onset of AD, and continue to increase linearly as a function of AD pathologic severity ($p<0.0001$).

Keywords

Alzheimer's disease; RAGE; Blood-brain barrier; Hippocampus; β-amyloid peptide; Microvessels

Author to whom correspondence should be addressed: Edward G. Stopa, MD, Division of Neuropathology, Department of Pathology, Rhode Island Hospital, 593 Eddy Street (APC 12-219), Providence, RI 02903, USA, Tel.: 1 (401) 444-5155, Fax: 1 (401) 444-8514, E-mail address: EStopa@lifespan.org.

1. INTRODUCTION

Amyloid-β peptide (Aβ) burden is a hallmark feature of Alzheimer's disease (AD) [Wisniewski et al. 1997; Hardy 2006; Deane and Zlokovic 2007; Haass and Selkoe 2007]. As a result, its questionable source has been a key area of interest. Historically, it has been proposed that cerebral Aβ is neuronal in origin [Masters et al. 1985], and that reactive astrocytes may also make a contribution [Siman et al. 1989]. However, growing evidence suggests that Aβ may stem from an even greater variety of sources, one of which may be receptor-mediated transport across the blood-brain barrier (BBB) [Zlokovic et al. 1993, Vitek et al. 1994, Poduslo et al. 1999]. RAGE, the human receptor for advanced glycation end-products, is a member of the immunoglobulin superfamily of cell surface molecules that binds candidates such as advanced glycation end-products and Aβ [Sasaki et al. 2001, Deane et al. 2003]. Because of its molecular structure and nature, RAGE has been under scrutiny for its potential role in mediating circulating plasma Aβ across the BBB and into the brain, where its deposition is seen in AD pathogenesis [Deane et al. 2003]. The direction of transport of Aβ by RAGE is of key interest, as it is in direct contrast to the outward-going movement of Aβ from the brain, across the blood-brain barrier, and into the plasma by way of other well-known receptors such as the low density lipoprotein receptor-related protein 1 (LRP-1) and P-glycoprotein (P-gp) [Shibata et al. 2000, Cirrito et al. 2005].

It has been reported that RAGE is present at high levels during development, especially in the central nervous system, and that its levels decline during maturity in normal aging [Leclerc et al. 2007]. However, increased expression of RAGE is reported to be associated with several pathological states, including Alzheimer's disease, diabetic nephropathy, and immune/inflammatory reactions of the vessel walls [Sasaki et al. 2001]. The majority of data collected for age-related changes in RAGE expression has made use of animal models, with relatively little being collected from post-mortem human subjects until recently. In a previous published report [Donahue et al. 2006], we compared RAGE expression in advanced AD patients to aged normal controls. In humans, it is suggested that in advanced Braak and Braak stage V-VI AD [Braak and Braak 1991, Small 1998, Braak et al. 2006], hippocampal neuronal RAGE immunoreactivity is faint compared to aged controls, while microvascular RAGE immunoreactivity is significantly increased compared to aged controls [Donahue et al. 2006]. The goal of this investigation is to quantify changes in human RAGE expression as they may relate to AD pathogenesis by establishing a continuum of normal aged controls without evident AD pathology, early AD pathology, and advanced AD samples. Our intent is to assess whether changes in RAGE precede or coincide with the appearance of AD-like pathology. Unlike our previous investigation in which optical density was assessed, in this study, a novel approach was utilized in which we calculated an average surface area of microvascular immunoreaction product across each sample per group as our mode of analysis using previously published methodologies [Wu et al. 1997, Stopa et al. 2008].

2. RESULTS

Distribution of 6E10 amyloid immunoreactivity

To verify the pathological diagnoses of the subjects used, we examined each case for the presence of senile plaques using a 6E10 amyloid immunostain. While both groups with AD pathology show signs of plaques and amyloid deposition, cases with advanced AD pathology have mature plaques with much more robust staining (Figure 1C), when compared to controls (Figure 1A) and cases with early AD pathology (Figure 1B).

Distribution of RAGE immunoreactivity

RAGE immunoreactivity was seen in early AD subjects, advanced AD subjects, and aged controls using low power magnified survey shots of the stained tissue sections. Representative samples from each group are shown in Figure 2. Both neurons and microvascular endothelial cells from the CA1 region of the hippocampus were positively stained for RAGE (Figures 3 and 4). In advanced AD, on average, we witnessed a strong RAGE signal in the microvasculature, while a notably weaker signal was seen in the microvasculature of both early AD and aged control patients (Figure 2). Hence, microvascular RAGE expression was notably upregulated in advanced AD when compared to early AD and control samples. It is also worth noting that microvascular RAGE staining in patients with early AD pathology appeared more robust optically than in the aged controls (Figure 2). As for neuronal RAGE expression in the CA1 region of the hippocampus, differences in number and expression were seemingly unremarkable on average across each group.

Double-labeling and co-localization studies

To confirm that RAGE staining was in fact present in the microvessels across all groups, we employed double-labeled fluorescent immunohistochemistry. We chose a common endothelial marker, CD-31, with which RAGE could be double-labeled. Co-localization was seen, with a representative photograph shown in Figure 3. For confirmation of RAGE staining in neurons, we double-labeled RAGE with neurofilament (Figure 4).

When probing through advanced AD cases, it is important to note that when examining neuritic plaques, no co-localization was evident between RAGE and Aβ in either the plaques or the vessels (Figure 5). However, there is high signal for RAGE in the vessels (red) and high signal for Aβ in the plaques (green).

Quantitative immunohistochemical analyses

The gradation of staining varied across the three groups (Figure 6), as supported by the calculated areas of immunoreaction product on microvascular endothelia. The raw surface area measurements, expressed in square microns, are shown in TABLE 1. A graphical representation of the data is given via a boxplot (Figure 7), depicting a quantitative difference in RAGE immunoreactivity in the microvascular endothelia across the control, early AD pathology, and advanced AD pathology subjects. From these data, a significant increase ($p=0.0001$) in endothelial RAGE immunoreactivity was found in severe AD patients when compared to aged controls, supporting our previous findings [Donahue et al. 2006]. In addition, a significant increase in endothelial RAGE immunoreactivity was found in severe Braak V-VI AD patients when compared to individuals with early AD pathology ($p=0.0125$), and in individuals having early AD-like pathology when compared to aged controls having no reported AD pathology ($p=0.038$). Looking at the entire continuum of groups using one-way ANOVA, a significant difference in endothelial RAGE surface area was also indicated among the three groups [F-value = 14.24 with associated p-value less than 0.001, d.f. (numerator) = 2 and d.f. (denominator) = 15]. There were no significant differences in age ($p=0.4670$), brain weight ($p=0.5612$), or postmortem interval ($p=0.9068$) among the control, early AD, or advanced AD groups. There were 8 females and 10 males, and there was no difference in mean RAGE immunoreactivity across the sexes ($p=0.9780$). An increasing linear trend in mean RAGE across controls, early AD, and advanced AD pathology was examined using linear contrast ($p<0.0001$), indicating evidence of a positive linear effect of RAGE immunoreactivity.

3. DISCUSSION

Aβ accumulation in the brains of AD patients and the mechanism behind its origin has garnered much attention in recent years. It has been postulated that the source of this pathology could

stem from alterations in the influx and efflux of Aβ at the site of the blood-brain barrier [Deane et al. 2003] in conjunction with reduced CSF clearance and rate of production noted in AD [Selkoe et al. 2000, Silverberg et al. 2001, Silverberg et al. 2003]. RAGE has been characterized as a transporter of Aβ from the plasma and into the brain via the blood-brain barrier [Deane et al. 2003, Deane et al. 2004]. That being said, an increase in RAGE expression in conjunction with AD severity could be physiologically too much to overcome, given the already reduced CSF turnover in AD [Silverberg et al. 2001].

The data that we collected support the general hypothesis that hippocampal microvascular RAGE immunoreactivity increases in advanced AD in human patients [Yan et al. 1996; Donahue et al. 2006]. In contrast to previous studies, we were able to provide a comparison of RAGE expression at very early versus advanced stages of Braak AD pathology. Our data suggests that RAGE is upregulated in the microvascular endothelium as the Braak stage of AD pathology increases. We used surface area calculations in this study, which are consistent with the microvascular optical density measurements in the advanced AD and control subjects used in our previous study [Donahue et al. 2006].

Our data show a significant difference between severe AD and controls, severe AD and early AD, and early AD and controls. Seeing statistical significance in this small sample size holds favorably for a trend toward increased RAGE surface area in patients with AD pathology, and suggests that increased RAGE levels may coincide with the onset of AD. Although Aβ is normally cleared in plasma, our data suggest that age-related hepatic insufficiency [Fisman 1990] combined with compromised CSF clearance and BBB integrity may initially lead to compromised Aβ clearance and resultant RAGE-mediated brain Aβ deposition. Because RAGE has been identified as a BBB influx transporter of soluble Aβ peptides, of which the blood is a major source, RAGE is becoming a significant therapeutic target in the treatment of AD [Zlokovic 2008]. Seeing as our data suggest that changes in RAGE expression at the BBB coincide with the onset of AD, use of RAGE blockers may have a role in early intervention and treatment of AD. A worthwhile future direction would be a replication of the same morphometric methods for other BBB-associated receptors such as LRP-1 and Pgp that been shown to transport Aβ in a manner opposite to that of RAGE, as overall regulation of Aβ in the brain is not restricted to just influx, but rather a combination of both influx and efflux transport [Zlokovic 2008].

4. EXPERIMENTAL PROCEDURE

Human brain tissue

Brains from 18 different individuals were examined in this study: 6 normal aged controls, 6 with early AD pathology (less than Braak and Braak stage III), and 6 with advanced AD pathology (Braak and Braak stage V–VI). Pathological and demographic data associated with each individual can be found in Table 2. None of the aged controls had evidence of clinical dementia or any AD neurofibrillary tangle pathology. One of the 6 individuals in the early AD pathology group had evidence of mild cognitive impairment; the remainder showed no evidence of clinical dementia. All of the patients from the severe Braak V–VI group fulfilled the NIA-Reagan criteria for Alzheimer's disease [Trojanowski et al. 1997]. Post-mortem human hippocampal tissue samples were excised and fixed in a 4% paraformaldehyde solution in 0.4M Sorensen's Phosphate buffer (pH 7.2) for 24 hours. Samples were then rinsed in phosphate buffer and placed in 30% sucrose in 0.1M Sorensen's phosphate buffer (pH 7.4) until sunken and cryoprotected.

RAGE Immunohistochemistry (free-floating)

Specimens were snap frozen in liquid nitrogen, embedded in OCT compound, and cryo-sectioned at a thickness of 50 microns. After a quick rinse in Tris-buffered saline (TBS), sections were quenched in 30% hydrogen peroxide for 10 minutes to block endogenous peroxidase activity, followed by a 48 hour blocking period with 5% normal rabbit serum at 4° C. After an overnight incubation (at 4°C) in a goat polyclonal anti-human RAGE antibody (Research Diagnostics, Flanders, NJ, USA), diluted 1:400, tissue sections were washed with TBS prior to application of the secondary antibody. For the secondary antibody, a rabbit anti-goat IgG (Vector Laboratories, Burlingame, CA, USA) was applied for 30 minutes at room temperature, diluted 1:500. The ABC detection system (Vector Laboratories, Burlingame, CA, USA) was utilized, and the tissue sections were stained using 3,3-diaminobenzidine (Vector Laboratories, Burlingame, CA, USA) as the chromogen. Sections were mounted on glass slides with the aid of a 1% gelatin solution and air dried overnight to dehydrate the tissue. Slides were coverslipped and sealed using Cytoseal, a xylene-based mounting medium (Stevens Scientific, Riverdale, NJ, USA). Primary antibody omission controls were run alongside the other samples to check for non-specific binding due to the secondary antibody. Immunoblotting was previously performed using this antibody to confirm specificity for RAGE [Donahue et al. 2006].

6E10 Amyloid Immunohistochemistry

Formalin-fixed paraffin embedded hippocampal tissue sections 10 μm in thickness were incubated in an oven at 60°C for one hour, and then deparaffinized and rehydrated. Tissue preparations were pretreated with 70% formic acid at room temperature for 10 minutes, followed by three thorough distilled water washes. Sections were quenched with 3% H_2O_2 and 50% methanol diluted in distilled water for 10 minutes. Non-specific binding sites were blocked by incubation with 5% normal horse serum for two hours at room temperature prior to incubation with the primary antibody (monoclonal mouse anti-human Aβ clone 6E10 antibody, Calbiochem, San Diego, CA, USA) overnight at 4°C. The tissue sections were then subjected to a modified ABC technique using the Vectastain Elite ABC Mouse Peroxidase system (Vector Laboratories, Burlingame, CA, USA) with 3,3-diaminobenzidine (Vector Laboratories, Burlingame, CA, USA) as the chromogen. Slides were coverslipped and sealed using Cytoseal, a xylene-based mounting medium (Stevens Scientific, Riverdale, NJ, USA).

Immunofluorescense

Specimens were snap frozen in liquid nitrogen, embedded in OCT compound, and cryo-sectioned at a thickness of 50 microns. After a quick rinse in TBS, sections were quenched in 30% hydrogen peroxide for 10 minutes to block endogenous peroxidase activity, followed by a 24 hour blocking period with 5% normal rabbit serum and normal horse serum at 4°C. Sections were incubated with antibodies directed against RAGE (1:400 dilution, Research Diagnostics, Flanders, NJ, USA), neurofilament (1:100 dilution, Novocastra, Newcastle, UK), and CD-31 (1:100 dilution, Research Diagnostics, Flanders, NJ, USA) in various combinations overnight at 4°C. After a TBS wash, sections were double-labeled with secondary antibodies conjugated to either Cy-2 or Cy-3 (Jackson ImmunoResearch, West Grove, PA, USA) at room temperature in the dark for one hour. To eliminate possible autofluorescense resulting from lipofuscin, tissue sections were incubated in a 0.3% Sudan Black B (Sigma-Aldrich, St. Louis, MO, USA) solution in 70% ethanol for 30 minutes at room temperature in the dark [Schnell et al. 1999]. In addition, certain specimens were histologically stained with a 0.1% Thioflavin S (Sigma-Aldrich, St. Louis, MO, USA) solution (made in 70% ethanol) for 30 minutes at room temperature in the dark. Thioflavin S, a fluorescent dye, was used to detect beta-amyloid deposition and also to confirm pathological diagnoses of the cases studied.

Image Analysis

For sections having DAB as the chromogen, grayscale images were obtained using a Nikon E800 microscope (Nikon Inc., Mellville, NY, USA) using a 60X objective. Images were acquired with a Spot II digital camera (Diagnostic Images, Sterling Heights, MI, USA) using the camera's auto-exposure. Ten random fields were analyzed per specimen to confirm the presence of RAGE in relation to capillary endothelia. Cross sections of cerebral microvessels 5–20 μm in diameter were selected out of the ten random field images acquired per specimen for analysis. Image processing and analysis was performed using NIH Image shareware (National Institute of Health, Springfield, VA, USA) along with previously reported methods [Wu et al. 1997, Stopa et al. 2008]. For surface area calculations, all images were thresholded by the same user at a single sitting in attempt to best reduce the error associated with this mode of analysis. Using the collected surface areas of capillary endothelial immunoreaction product, statistics were performed. A one-way analysis of variance was used to test for differences in mean microvascular RAGE surface area measurements across all three groups (control, early AD, and advanced AD) and Tukey's test for multiple comparisons was used to test for all pairwise differences among groups (controls and early AD, controls and advanced AD, and early AD and advanced AD). The statistical software SAS (version 9.1) and Microsoft Excel was used in the statistical analyses. For confocal microscopy, samples were optically sectioned with a Nikon PCM 2000 microscope (Nikon Inc., Mellville, NY, USA) using the Argon (488) and the Helium-Neon (543) lasers. Images were acquired with a Spot II digital camera (Diagnostic Images, Sterling Heights, MI, USA).

Acknowledgements

This work was supported by NIH R01 AG027910 (awarded to C.E.J.), a Temporal Discovery Award granted to E.G.S. and C.E.J. by the Alzheimer's Association, the Rae and Jerry Richter Fund (at the Neurosurgery Foundation, Brown University, Providence, RI), and the Saunders Family Fund (at the Neurosurgery Foundation, Brown University, Providence, RI). The authors wish to thank Victoria Kuo and Stephanie Slone for their contributions, as well as the Brown University Brain Tissue Resource Center.

ABREVIATIONS

Aβ
: amyloid-β peptide

AD
: Alzheimer's disease

RAGE
: receptor for advanced glycation end-products

BBB
: blood-brain barrier

LRP-1
: low density lipoprotein receptor-related protein 1

P-gp
: P-glycoprotein

LITERATURE REFERENCES

Braak H, Braak E. Neuropathological staging of Alzheimer-related changes. Acta Neuropathol 1991;82:239–259. [PubMed: 1759558]

Braak H, Alafuzoff I, Arzberger T, Kretzschmar H, Del Tredici K. Staging of Alzheimer disease-associated neurofibrillary pathology using paraffin sections and immunohistochemistry. Acta Neuropathol 2006;112:389–404. [PubMed: 16906426]

Cirrito JR, Deane R, Fagan AM, Spinner ML, Parsadanian M, Finn MB, Jiang H, Prior JL, Sagare A, Bales KR, Paul SM, Zlokovic BV, Piwnica-Worms D, Holtzman DM. P-glycoprotein deficiency at the blood-brain barrier increases amyloid-beta deposition in an Alzheimer disease mouse model. J Clin Invest 2005;115(11):3285–3290. [PubMed: 16239972]

Deane R, Yan SD, Sunmamaryan RK, LaRue B, Jovanovic S, Hogg E, Welch D, Manness L, Lin C, Yu J, Zhu H, Ghiso J, Frangione B, Stern A, Schmidt A, Armstrong DL, Arnold B, Liliensiek B, Nawroth P, Hofman F, Kindy M, Stern D, Zlokovic B. RAGE mediates amyloid β-peptide across the blood-brain barrier and accumulation in the brain. Nature Medicine 2003;9:907–913.

Deane R, Wu Z, Zlokovic BV. RAGE (yin) versus LRP (yang) balance regulates alzheimer amyloid-beta peptide clearance through transport across the blood-brain barrier. Stroke 2004;35:2628–2631. [PubMed: 15459432]

Deane R, Zlokovic BV. Role of blood brain barrier in the pathogenesis of Alzheimer's disease. Curr Alzheimer Res 2007;4:191–197. [PubMed: 17430246]

Donahue JE, Flaherty SL, Johanson CE, Duncan JA 3rd, Silverberg JD, Miller MC, Tavares R, Yang W, Wu Q, Sabo E, Hovanesian V, Stopa EG. RAGE, LRP-1, and amyloid-beta protein in Alzheimer's disease. Acta Neuropathol (Berl) 2006;112:405–415. [PubMed: 16865397]

Fisman M. Hepatic aging as an etiological factor in the development of Alzheimer's disease. Med Hypotheses 1990;33(3):163–167. [PubMed: 2292979]

Haass C, Selkoe DJ. Soluble protein oligomers in neurodegeneration: lessons from the Alzheimer's amyloid beta-peptide. Nat Rev Mol Cell Biol 2007;8:101–112. [PubMed: 17245412]

Hardy J. A hundred years of Alzheimer's disease research. Neuron 2006;52:3–13. [PubMed: 17015223]

Leclerc E, Fritz G, Weibel M, Heizmann CW, Galichet A. S100B and S100A6 Differentially Modulate Cell Survival by Interacting with Distinct RAGE (Receptor for Advanced Glycation End Products) Immunoglobulin Domains. J Biol Chem 2007;282:31317–31331. [PubMed: 17726019]

Masters CL, Multhaup G, Simms G, Pottgiesser J, Martins RN, Beyreuther K. Neuronal origin of a cerebral amyloid: neurofibrillary tangles of Alzheimer's disease contain the same protein as the amyloid of plaque cores and blood vessels. EMBO J 1985;4(11):2757–2763. [PubMed: 4065091]

Mirra SS, Heyman A, McKeel D, Sumi SM, Crain BJ, Brownlee LM, Vogel FS, Hughes JP, van Belle G, Berg L. participating CERAD neuropathologists. The consortium to establish a registry for Alzheimer's disease (CERAD): Part II Standardization of the neuropathological assessment of Alzheimer's disease. Neurology 1991;41:479–486. [PubMed: 2011243]

Poduslo J, Curran G, Sanyal B, Selkoe D. Receptor-mediated transport of human amyloid beta-protein 1–40 and 1–42 at the blood-brain barrier. Neurobiol Dis 1999;6(3):190–199. [PubMed: 10408808]

Sasaki N, Toki S, Chowei H, Saito T, Nakano N, Hayashi Y, Takeuchi M, Makita Z. Immunohistochemical distribution of the receptor for advanced glycation end products in neurons and astrocytes in Alzheimer's disease. Brain Res 2001;888(2):256–262. [PubMed: 11150482]

Schnell SA, Staines WA, Wessendorf MW. Reduction of lipofuscin-like autofluorescence in fluorescently labeled tissue. J Histochem Cytochem 1999;47:719–730. [PubMed: 10330448]

Selkoe DJ. Toward a comprehensive theory for Alzheimer's disease. Hypothesis: Alzheimer's disease is caused by the cerebral accumulation and cytotoxicity of amyloid beta-protein. Ann NY Acad Sci 2000:92417–92425.

Silverberg GD, Heit G, Huhn S, Jaffe RA, Chang SD, Bronte-Stewart H, Rubenstein E, Possin K, Saul TA. The cerebrospinal fluid production rate is reduced in dementia of the Alzheimer's type. Neurology 2001;57(10):1763–1766. [PubMed: 11723260]

Silverberg GD, Mayo M, Saul T, Rubenstein E, McGuire D. Alzheimer's disease, normal-pressure hydrocephalus, and senescent changes in CSF circulatory physiology: a hypothesis. Lancet Neurol 2003;2(8):506–511. [PubMed: 12878439]

Siman R, Card JP, Nelson RB, Davis LG. Expression of beta-amyloid precursor protein in reactive astrocytes following neuronal damage. Neuron 1989;3(3):275–285. [PubMed: 2518369]

Shibata M, Yamada S, Kumar SR, Calero M, Bading J, Frangione B, Holtzman DM, Miller CA, Strickland DK, Ghiso J, Zlokovic BV. Clearance of Alzheimer's amyloid-β_{1-40} peptide from brain by LDL

receptor-related protein-1 at the blood-brain barrier. J Clin Invest 2000;106(12):1489–1499. [PubMed: 11120756]

Small GW. The pathogenesis of Alzheimer's Disease. J Clin Psychiatry 1998;59(Supplement 9):7–14. [PubMed: 9720481]

Stopa EG, Butala P, Salloway S, Johanson CE, Gonzalez L, Tavares R, Hovanesian V, Hulette CM, Vitek MP, Cohen RA. Cerebral cortical arteriolar angiopathy, vascular beta-amyloid, smooth muscle actin, Braak stage, and APOE genotype. Stroke 2008;39(3):814–821. [PubMed: 18258839]

Trojanowski JQ, Clark CM, Schmidt ML, Arnold SE, Lee VM. Strategies for improving the postmortem neuropathological diagnosis of Alzheimer's disease. Neurobiol Aging 1997;18(4 Suppl):S75–S79. [PubMed: 9330990]

Vitek MP, Bhattacharya K, Glendening JM, Stopa E, Vlassara H, Bucala R, Manogue K, Cerami A. Advanced glycation end products contribute to amyloidosis in Alzheimer disease. Proc Natl Acad Sci USA 1994;91(11):4766–4770. [PubMed: 8197133]

Wisniewski T, Ghiso J, Frangione B. Biology of Aβ amyloid in Alzheimer's disease. Neurobiol Dis 1997;4:311–328.

Wu LC, D'Amelio F, Fox RA, Polyakov I, Daunton NG. Light microscopic image analysis system to quantify immunoreactive terminal area apposed to nerve cells. J Neurosci Methods 1997;74:89–96. [PubMed: 9210578]

Yan SD, Chen X, Fu J, Chen M, Zhu H, Roher A, Slattery T, Zhao L, Nagashima M, Morser J, Migheli A, Nawroth P, Stern D, Schmidt AM. RAGE and amyloid-beta peptide neurotoxicity in Alzheimer's disease. Nature 1996;382(6593):685–691. [PubMed: 8751438]

Zlokovic BV, Ghiso J, Mackic JB, McComb JG, Weiss MH, Frangione B. Blood-brain barrier transport of circulating Alzheimer's amyloid beta. Biochem Biophys Res Commun 1993;197(3):1034–1040. [PubMed: 8280117]

Zlokovic BV. The blood-brain barrier in health and chronic neurodegenerative disorders. Neuron 2008;57(2):178–201. [PubMed: 18215617]

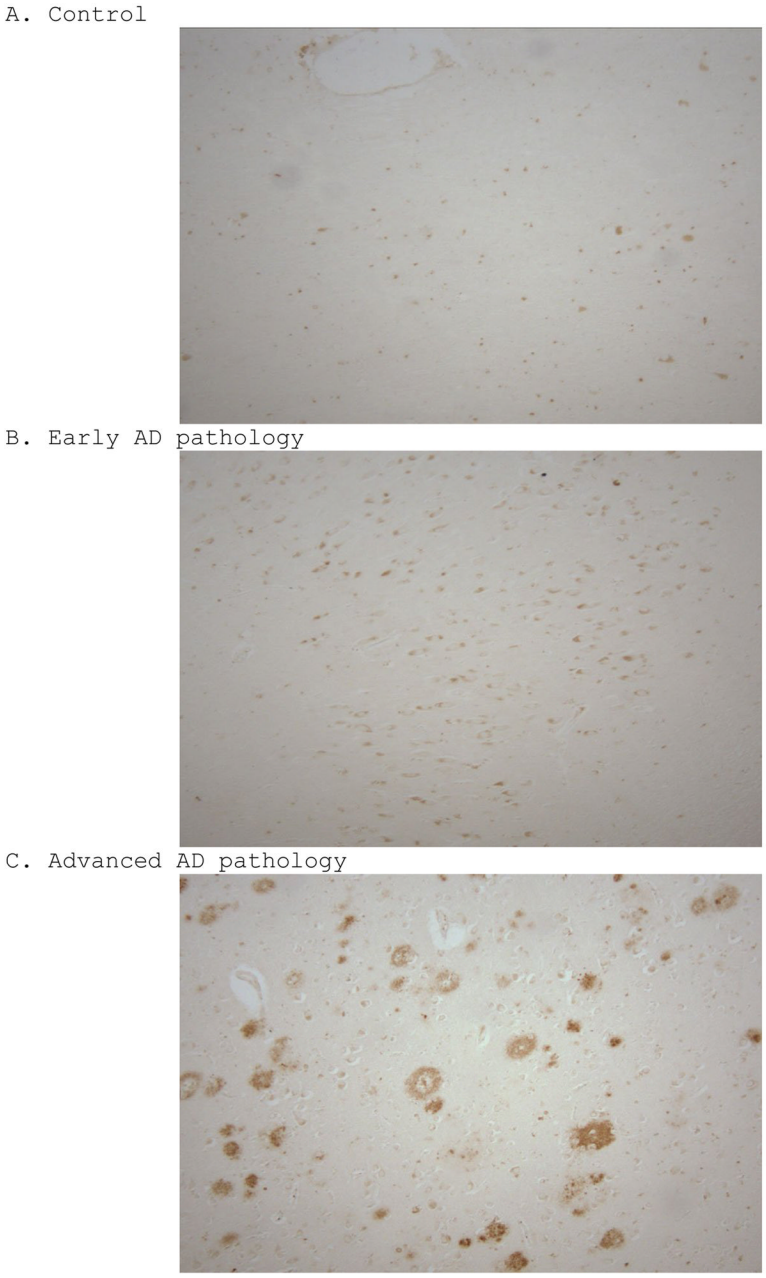

Figure 1.
6E10 amyloid immunohistochemical staining on control (A), early AD (B), and advanced AD (C) cases, showing a progressive trend in Aβ deposition. Each photograph is of a 100X magnification.

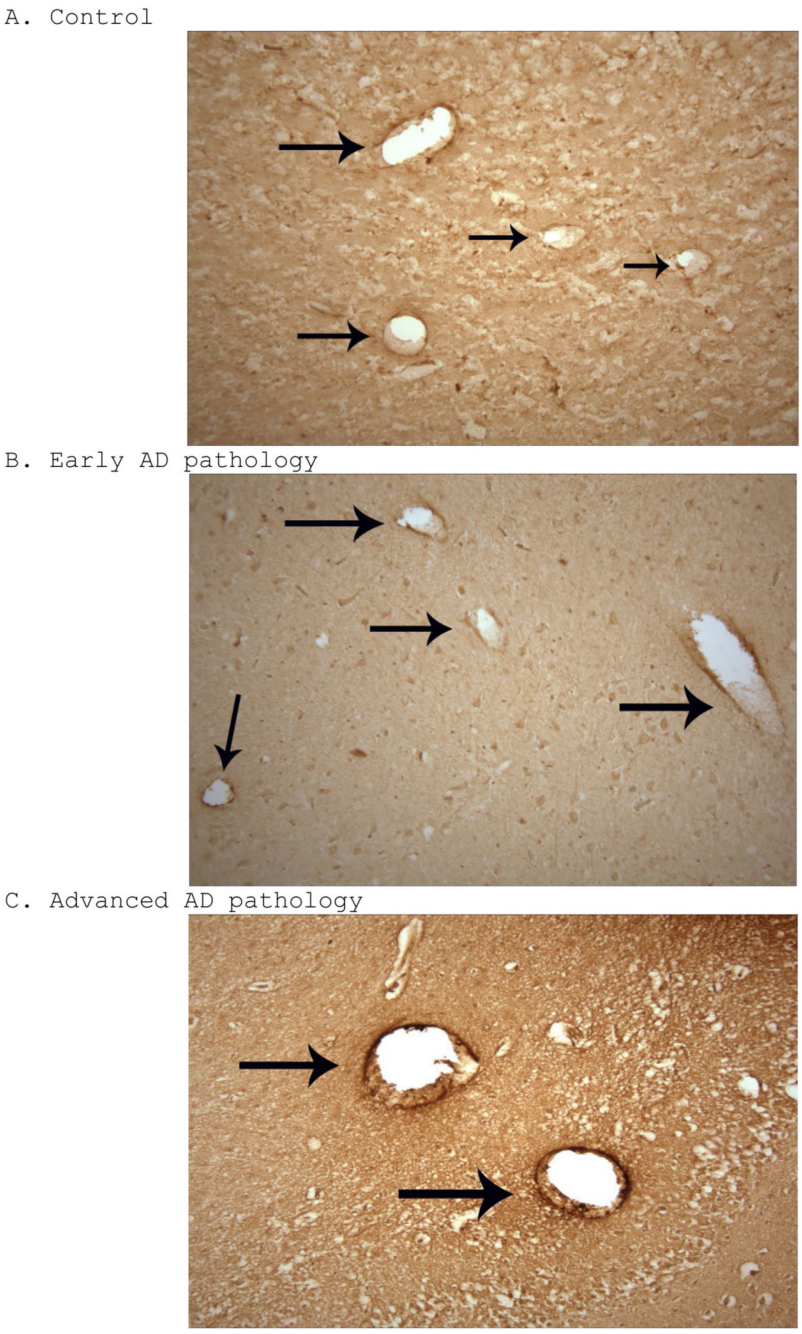

Figure 2.
RAGE immunohistochemical staining, shown 100X, on control (A), early AD (B), and advanced AD (C) cases, with arrows pointing to RAGE immunoreactivity in vessel walls. There is a trend toward increased microvascular RAGE immunoreactivity across the continuum of the three groups.

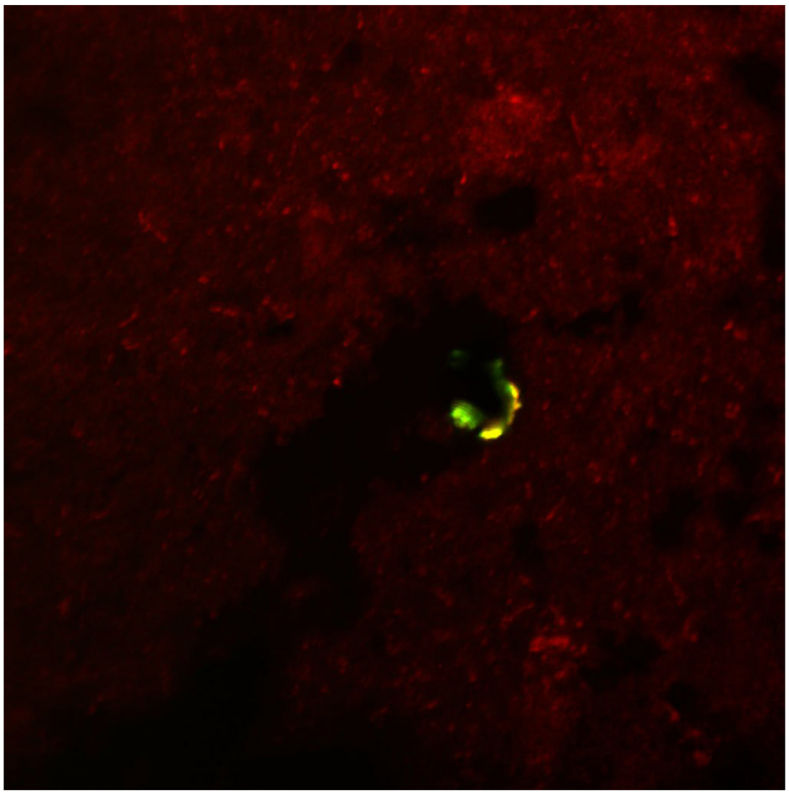

Figure 3.
Section of human AD hippocampus double-labeled with RAGE (red) and CD-31 (green). Shown is a merged image (600X) showing colocalization of RAGE and CD-31 in the microvasculature (yellow staining).

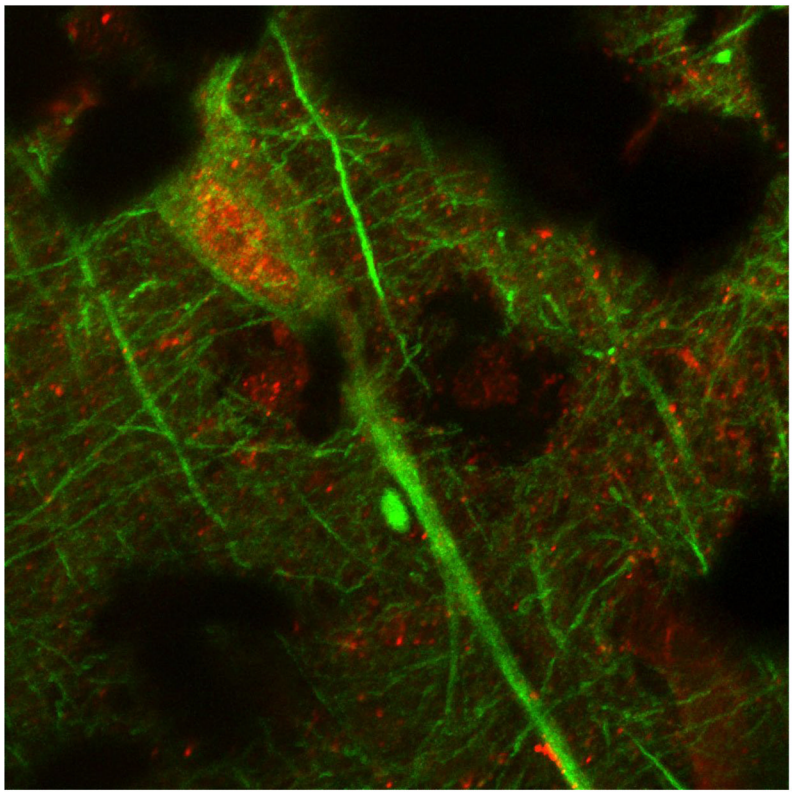

Figure 4.
Section of human control hippocampus double-labeled with RAGE (red) and neurofilament (green). Shown is merged image (600X) depicting a sample neuron.

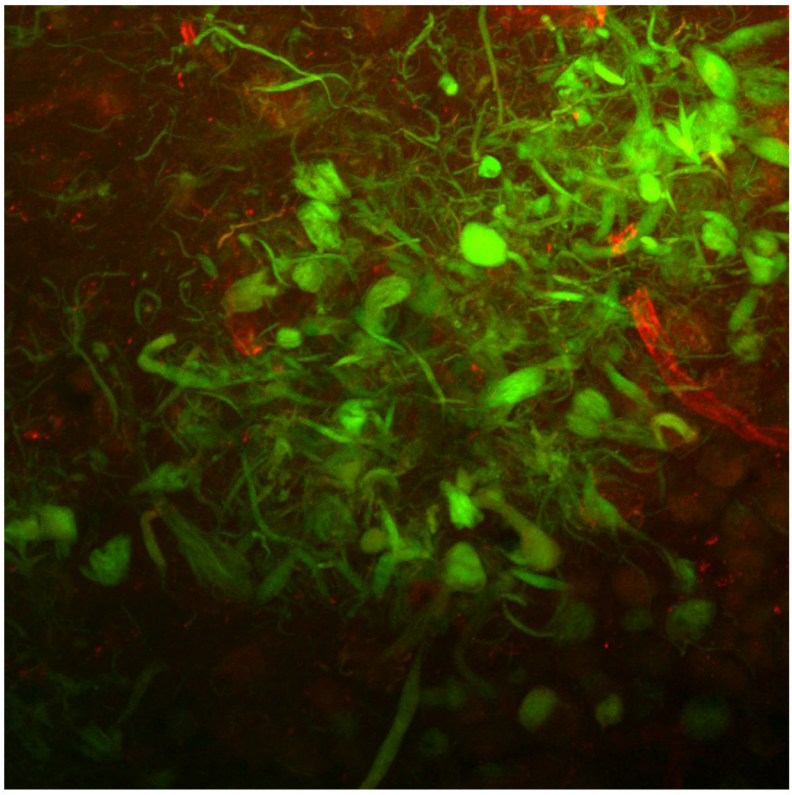

Figure 5.
Section of human AD hippocampus double-labeled with RAGE (red) and Thioflavin S (green). Shown is a merged image (600X) showing no colocalization of RAGE and CD-31 in the senile plaque depicted.

A. Control

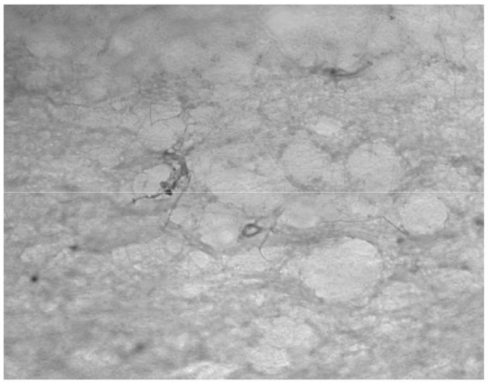

B. Early AD pathology

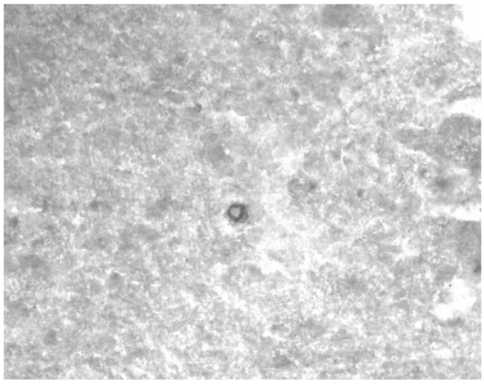

C. Advanced AD pathology

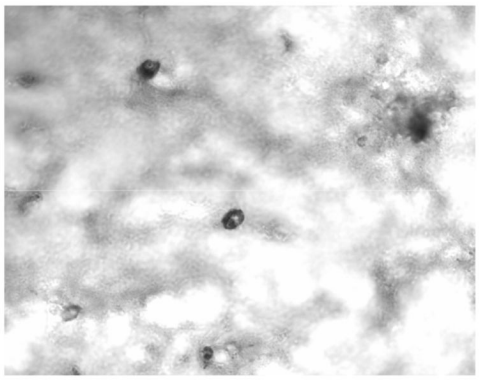

Figure 6.

Sections of human hippocampi (600X) stained with RAGE used in quantitative analyses. The detection system is ABC (Vector Laboratories) with 3,3-diaminobenzidine as the chromogen. RAGE immunoreactivity is weak to moderate in hippocampal microvasculature in aged control samples (A), moderate in cases with early AD pathology (B), and robust in cases with advanced AD pathology (C).

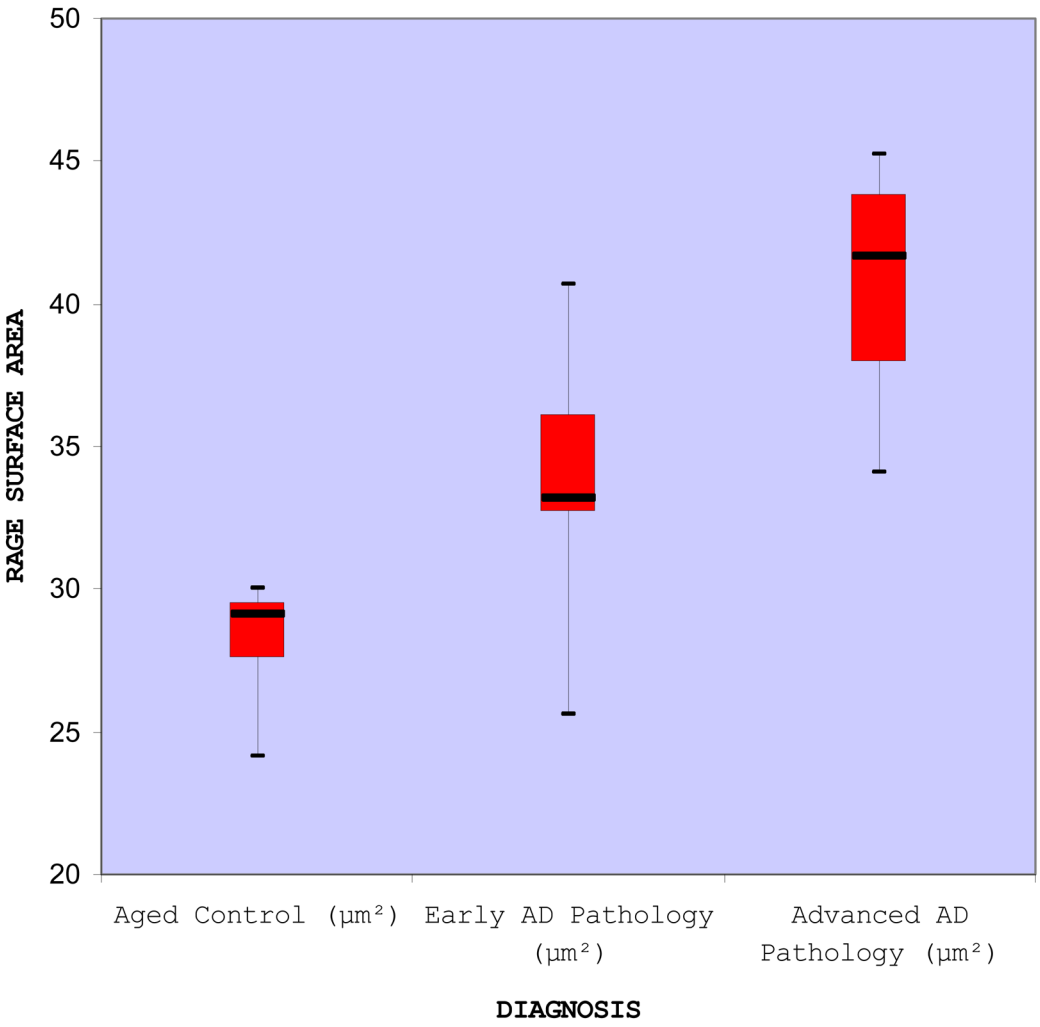

Figure 7.
Summary of RAGE surface area measurements. The boxplots display the median (middle dark line), the lower (25th percentile) and upper (75th percentile) quartiles, lines delimiting the boxes, and the maximum and minimum value of the data sets, as indicated by the whiskers in the plot.

TABLE 1

Quantitative immunohistochemical surface areas in the microvasculature for RAGE in control, early AD, and advanced AD hippocampi.

Control (μm^2)	Early AD pathology (μm^2)	Advanced AD pathology (μm^2)
24.17	32.71	43.37
29.29	33.67	39.94
27.07	36.95	34.11
29.57	40.71	45.22
30.05	25.58	37.28
28.99	32.73	43.95

Table 2

Summary of clinical and pathological data, including age, sex, post-mortem interval (PMI), brain weight (in grams), classification for the study (control, early AD, or advanced AD), Braak stage (Braak and Braak 1991, Braak et al. 2006), CERAD score (Mirra et al. 1991), and clinical diagnosis (cause of death).

Case	Age (years)	Sex	Post-mortem interval (PMI)	Brain weight (g)	Classification	Braak stage	CERAD score	Clinical diagnosis (cause of death)
1	63	Male	19	1550	Control	No NT pathology	Absent (0)	Coronary artery disease; right tibial osteomyelitis
2	66	Female	14	1280	Control	No NT pathology	Absent (0)	Pancreatic carcinoma
3	74	Male	24.5	1219	Control	No NT pathology	Absent (0)	Glioblastoma
4	77	Male	16	1183	Control	No NT pathology	A	Coronary artery disease; atherosclerosis
5	63	Female	19	1209	Control	No NT pathology	Absent (0)	Abdominal metastatic carcinoma
6	86	Male	13	1349	Control	No NT pathology	A	Hydrocephalus → SDH after shunt
7	82	Female	13	1175	Early AD	Stage I	A	Metastatic adenocarcinoma (lung); respiratory insufficiency
8	91	Male	20	1364	Early AD	Stage I	B	Pneumonia; renal failure
9	72	Male	24	1200	Early AD	Stage I	C	Cardiac arrhythmia; mild cognitive impairment
10	68	Female	9	1074	Early AD	Stage I	B	Retroperitoneal tumor
11	70	Female	21	1249	Early AD	Stage I	B	Metastatic squamous cell carcinoma (lung)
12	77	Male	7	1080	Early AD	Stage II	B	Multiple myeloma
13	66	Female	2.5	900	Advanced AD	Stage V	C	Alzheimer’s disease; severe atherosclerosis; pneumonia
14	77	Male	9.2	1300	Advanced AD	Stage V	C	Alzheimer’s disease; hypertension; COPD
15	74	Female	12	1350	Advanced AD	Stage V	C	Alzheimer’s disease; melanoma
16	73	Male	8	1350	Advanced AD	Stage V	C	Alzheimer’s disease; atherosclerosis
17	77	Female	10	1093	Advanced AD	Stage V	C	Alzheimer’s disease; pneumonia
18	63	Male	48	1653	Advanced AD	Stage VI	C	Alzheimer’s disease; acute renal failure